

Code Design for Discrete Memoryless Interference Channels

Mehdi Dabirnia, *Member, IEEE*, A. Korhan Tanc, *Member, IEEE*, Shahrouz Sharifi, and Tolga M. Duman[✉], *Fellow, IEEE*

Abstract—We study the design of explicit and implementable codes for the two-user discrete memoryless interference channels (DMICs). We consider Han–Kobayashi (HK) type encoding where both public and private messages are used and propose coding techniques utilizing a serial concatenation of a nonlinear trellis code (NLTC) with an outer low-density parity-check (LDPC) code. Since exact analytical treatment of the BCJR decoder for the inner trellis-based code appears infeasible, we analytically investigate the iterative decoding process in the asymptotic regime where the probability of decoding error tends to zero. Based on this approximate analysis, we derive a stability condition for this type of a concatenated coding scheme for the first time in the literature. Furthermore, we use an extrinsic information transfer analysis to design the outer LDPC code while fixing the inner NLTC, and utilize the derived stability condition to accelerate the design process and to avoid code ensembles that potentially produce high error floors. Via numerical examples, we demonstrate that our designed codes achieve rate pairs close to the optimal boundary of the HK subregion, which cannot be obtained without the use of nonlinear codes. Also, we verify that the estimated thresholds of the designed codes via finite block length simulations and show that our designs significantly outperform the point-to-point optimal codes, hence demonstrating the need for designs specifically tailored for DMICs.

Index Terms—Discrete memoryless interference channels, nonlinear trellis codes, low-density parity-check codes, concatenated codes, stability condition.

I. INTRODUCTION

AN interference channel (IC) is a communication medium shared by several sender-receiver pairs. Transmission of

Manuscript received September 6, 2017; revised February 8, 2018; accepted March 6, 2018. Date of publication March 19, 2018; date of current version August 14, 2018. This work was supported in part by the Turkish Scientific and Technological Research Council of Turkey under Grant 114E601, in part by the National Science Foundation under Grant NSF-CCF 1117174, and in part by the European Commission under Grant MC-CIG PCIG12-GA-2012-334213. An early version of this work was presented at the IEEE International Symposium on Information Theory, Hong Kong, June 2015. Part of this paper is based on the Ph.D. thesis of M. Dabirnia completed at Bilkent University [1]. The associate editor coordinating the review of this paper and approving it for publication was R. Thobaben. (*Corresponding author: Tolga M. Duman.*)

M. Dabirnia is with the Department of Electrical and Electronics Engineering, Bilkent University, 06800 Ankara, Turkey. He is now with the Department of Information and Communication Technologies, Universitat Pompeu Fabra, 08018 Barcelona, Spain (e-mail: mehdi.dabirnia@upf.edu).

A. K. Tanc is with the Department of Biomedical Engineering, Biruni University, 34020 Istanbul, Turkey (e-mail: atanc@biruni.edu.tr).

S. Sharifi is with Maxlinear, Carlsbad, CA 92008 USA (e-mail: ssharifi@maxlinear.com).

T. M. Duman is with the Department of Electrical and Electronics Engineering, Bilkent University, 06800 Ankara, Turkey (e-mail: duman@ee.bilkent.edu.tr).

Color versions of one or more of the figures in this paper are available online at <http://ieeexplore.ieee.org>.

Digital Object Identifier 10.1109/TCOMM.2018.2817233

information from each sender to its corresponding receiver interferes with the communication between the other sender and receiver pairs. Most of the existing studies on ICs focus on information theoretic problems while only a few works have been reported on designing practical and implementable codes. For instance, [2]–[4] consider code design for Gaussian interference channels (GICs) where low-density parity-check (LDPC) codes for the two user GICs for very large block lengths are considered, and it is shown that rate pairs close to the capacity or achievable rate region (ARR) boundaries are attainable. In another study, lattice codes along with underlying spatially coupled LDPC codes are shown to provide excellent performance for the three user symmetric GIC [5]. [6] considers a symmetric two-user GIC, and by employing LDPC codes and a different decoding approach for each interference region, obtains sum-rates close to the Han-Kobayashi (HK) limit. A coding scheme based on concatenation of a Kite code with a convolutional code is recently proposed in [7], and rate pairs close to the theoretical achievable rates have been obtained. It has also been shown that a decoding gain can be achieved by considering the structure of the interference. In this paper, our objective is to consider the case of generic discrete memoryless interference channels (DMICs), and design explicit and implementable codes for different scenarios as a complementary work to [2]–[7], which focus on the case of GICs. We note that beside its theoretical importance, the DMIC model has potential applications in optical communications with uncoordinated multi-user access [8] as well as in power efficient multi-user communication systems with low-bit analog-to-digital converters (ADCs) [9].

Determination of the DMIC capacity is still an open problem except for some special cases, e.g., strong ICs [10], [11], classes of degraded ICs [12], [13], and classes of deterministic and semideterministic ICs [14], [15]. Han and Kobayashi in [16] established an inner bound on the capacity region, which is still the best known ARR. In this scheme, each user splits its data into private and public messages, which are decoded at the intended receivers and both receivers, respectively. More recently, [17] derives the sum rate capacity of a DMIC with one-sided weak interference, and shows that in order to achieve this sum rate both users should transmit their information as private messages only, i.e., the receivers should decode their desired messages while treating the interference as noise.

Recent studies have investigated optimal transmission strategies for some instances of discrete memoryless multi-user channels. Xie *et al.* [18] present an optimal transmission

strategy for the broadcast Z channel with independent encoding and successive decoding. They employ nonlinear turbo codes with a desired distribution of ones and zeros in their codebook to operate close to the optimal rate region boundary. A capacity-achieving encoding scheme is designed for a general degraded binary broadcast channel (DBBC) in [19]. The designed scheme uses simple logical operators (i.e., XOR, OR and AND) at the output of independent binary encoders to achieve the capacity boundary. In [20], a relatively simple encoding scheme, which is called natural encoding, is shown to achieve the capacity of several classes of discrete memoryless degraded broadcast channels. Design of nonlinear trellis codes (NLTCs) for binary-input binary-output multiple access channels (MACs) has been investigated in [8] where a non-uniform distribution of ones and zeros is required. A polar coding scheme for the two user DMIC is introduced in [21] achieving the HK inner bound, which can be generalized to interference networks. [22] proposes a simplified design of polar codes to achieve the HK rate region for the two-user DMIC, which does not require mapping functions from auxiliary random variables to channel inputs. While these studies on the use of polar codes over DMICs show the asymptotic achievability of the HK inner bound, they do not provide explicit and implementable codes, which motivates our approach.

In this paper, we consider practical code design for different instances of DMICs. We employ an HK type encoding by considering private and public messages for both users. As a practical coding scheme, we propose a serial concatenation of a trellis based code (which can be an NLTC or a convolutional code depending on the required distribution for each message) with an outer LDPC code. In order to design the inner trellis based code we adopt an algorithm proposed in [23], which is based on maximizing the minimum distance of the code. Motivated by their excellent performance over various channels, we use irregular LDPC codes as the outer codes in the concatenated coding scheme. At the receiver side, we utilize an iterative decoder implementing Bahl, Cocke, Jelinek and Raviv (BCJR) algorithm over the extended trellis of the inner codes, and a component belief propagation decoder for each of the outer LDPC codes. Furthermore, we optimize the degree distribution of the outer LDPC codes via an instance of differential evolution [24], namely, the random perturbation technique armed with the extrinsic information transfer (EXIT) analysis. In some special cases, we also consider a simpler version of the proposed coding scheme by utilizing only private messages, or one user's message as public while the other is private.

Another main contribution of the paper is the development of a general stability condition for the concatenated coding scheme (over both symmetric and asymmetric channels), which is applicable more broadly than the present set-up. We utilize the derived stability condition to accelerate the LDPC code design process, and to avoid code ensembles that potentially produce high error floors. Through several examples, we explicitly show that our designed codes operate at rates close to the optimal rate region boundaries, and they significantly outperform the single user codes with

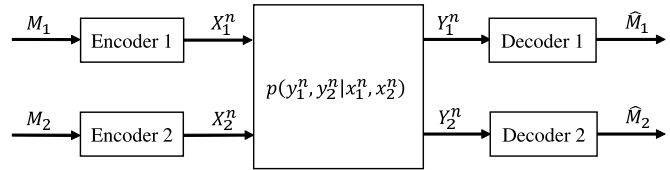


Fig. 1. Block diagram of the two-user interference channel.

time sharing. Additionally, we demonstrate that by utilizing the concatenated coding scheme with the inner NLTC, one can achieve rate pairs that cannot be obtained by linear codes alone.

The rest of the paper is organized as follows. In Section II, we describe the system model for a two-user DMIC. We explain the proposed coding scheme and elaborate on the code design process in Section III. We provide an asymptotic analysis of the concatenated coding scheme over both symmetric and asymmetric channels, and derive the stability condition for the convergence of the iterative decoder in Section IV. Section V includes three different sets of DMIC examples with several newly designed codes for each case. Concluding remarks are provided in Section VI.

II. SYSTEM MODEL

A two sender-receiver pair communication system is depicted in Fig. 1 where each sender wishes to send a message to its corresponding receiver over a shared interference channel. The discrete IC is specified by its finite input alphabets \mathcal{X}_1 and \mathcal{X}_2 , finite output alphabets \mathcal{Y}_1 and \mathcal{Y}_2 , and the channel transition probabilities

$$p(y_1|x_1x_2) = \sum_{y_2 \in \mathcal{Y}_2} p(y_1y_2|x_1x_2), \quad (1)$$

$$p(y_2|x_1x_2) = \sum_{y_1 \in \mathcal{Y}_1} p(y_1y_2|x_1x_2). \quad (2)$$

We also assume that the IC is memoryless, i.e.,

$$p(y_1^n y_2^n | x_1^n x_2^n) = \prod_{i=1}^n p(y_{1i} y_{2i} | x_{1i} x_{2i}) \quad (3)$$

where the subscript i denotes the time instant. The HK ARR for this channel can be found in [16] and [25, p 143].

III. PROPOSED CODING SCHEME

A. Encoding and Decoding

We consider practical code design for different instances of DMICs restricted to the case of binary inputs and binary outputs. We employ an HK type encoding, which transmits private and public messages for each user. Three messages (both intended messages and the public message of the other user) at each receiver are decoded. Since communication takes place over an IC, there is a tradeoff between the rates at which both users can reliably communicate. As a result, one may use different input distributions and obtain different optimal rate pairs on the boundary of the ARR. In order to operate at one of these points, a specific input distribution is required for each message, which is usually nonuniform. On the other hand, linear codes (e.g., LDPC codes) induce a

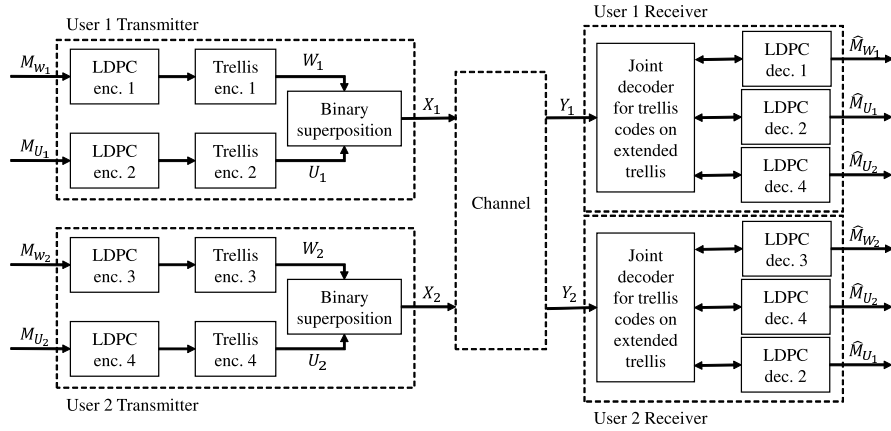


Fig. 2. Block diagram of the proposed coding scheme. W_i and U_i stand for private and public messages for user i , respectively.

uniform distribution of 0's and 1's, hence new approaches are needed for implementing channel coding solutions over ICs.

In order to obtain a good error correction performance and to generate the required nonuniform input distributions, we propose employing concatenation of an outer LDPC code with an inner nonlinear trellis code as a practical and implementable solution. Fig. 2 depicts the block diagram of the proposed coding scheme for a two-user IC. The transmitter side consists of concatenation of an outer LDPC code and an inner trellis based code for either one of the public and private messages of each user, which are then connected to the channel after superposition. The objective of the inner trellis based code is to introduce the required distribution at the channel input while also providing further protection against channel noise. For the cases where the optimal input distribution is uniform, we can remove the trellis based code, and employ only an LDPC code. At the receiver sides, BCJR algorithm based decoders operating over the product trellises of the NLTCs are adopted to compute the log-likelihood-ratios (LLRs) of the encoded bits, which are then iteratively exchanged with the respective LDPC decoders to improve the decoding performance.

While the general HK type encoding can be implemented using the proposed scheme, it is not necessary for certain special cases, and one may use simpler versions, e.g., by utilizing only private messages, or only public messages. We note that for the case of using only private messages and treating interference as noise at both decoders, the problem becomes similar to transmitting over a point-to-point asymmetric channel. This set-up has been studied in several papers, e.g., in [26] where three different approaches to achieve the capacity of asymmetric channels are introduced. We emphasize, however, that this work does not provide any explicit code design. We also note that the proposed scheme in this paper is more general as it provides a practical HK type coding solution for DMICs.

B. Inner NLTC Design

An NLTC design algorithm is developed in [23] with the goal of maximizing the minimum distance of the code while keeping a desired ones' density. Specifically, a finite-state shift

register is used to specify the state of the encoder and by shifting the input data into and along the shift register (from the left), the next state of the encoder and the corresponding transitions are determined. We do not go over the details of this design algorithm here, and refer the reader to [23]. The result of the design algorithm is a lookup table, which determines the assignment of the labels to the branches of the trellis. As we will discuss later in Section IV, having a larger minimum distance helps with the stability of the iterative decoding process and provides a lower error floor for the concatenated coding scheme. Therefore, we utilize this approach to design the inner NLTC needed in our scheme as well.

C. Outer LDPC Code Design

Due to the use of an inner code and the presence of interference, off-the-shelf LDPC codes that are optimized for point-to-point (P2P) communications may not be optimal in our set-up. That is, we need to design new LDPC codes for each specific scenario. After we fix the inner NLTC (as in the previous subsection), we optimize the degree distribution of the LDPC code ensemble. We can utilize different techniques such as density evolution (DE) or EXIT charts for analyzing the iterative decoder performance, and optimization approaches such as linear programming or random perturbation for code design.

DE introduced in [27] is a method to track the probability density functions (PDFs) of the exchanged LLRs in the belief propagation decoder analytically. However, an analytical treatment of the BCJR decoder is not feasible [28], and hence, it is not a reasonable choice for analyzing the behavior of the iterative decoding process for the proposed concatenated coding scheme. EXIT analysis is a method developed to track the evolution of the mutual information between the transmitted bits and the corresponding LLRs [28], which requires a significantly lower computational complexity. In this paper, we utilize an EXIT analysis without making any assumptions on the Gaussianity of the PDFs of the exchanged LLRs within the decoder. The only assumption is the symmetry of the PDFs of the exchanged LLR values among the component decoders defined as the condition $f(x) = e^x f(-x)$ for $x \in \mathbb{R}$.

As we will discuss in detail in Section IV, the LLR symmetry property is satisfied for the exchanged messages in the iterative decoding of the proposed class of concatenated codes, hence our approach is valid. However, the channel output symmetry, which enables us to consider transmission of the all-zero codeword is not valid for multi-user scenarios; and, in order to overcome this problem, we utilize independent and identically distributed (i.i.d.) channel adaptors with common randomness at the transmitter and receiver sides for each message [29]. We note that the i.i.d. channel adaptors are utilized for the sake of analysis only and they are neither needed nor utilized for the actual communication system. Then, we follow the approach taken in [30] and compute the extrinsic mutual information as

$$I(L; X) \approx 1 - \frac{1}{N} \sum_{n=1}^N \log_2(1 + e^{-L_n}) \quad (4)$$

with L_n denoting the LLR corresponding to the n th coded bit of the all-zero codeword.

Inspired by the results of [31], in order to get lower decoding thresholds, we select an initial degree distribution with multiple degrees at both variable and check node sides with a rate lower than the final goal such that it satisfies the stability condition. Using Monte Carlo simulations for sufficiently long block lengths (taken as 10^6 in this paper), and running the iterative decoding algorithm, we check the admissibility of the initial degree. More precisely, we track the evolution of the mutual information at the output of the variable node decoder (VND) and the check node decoder (CND), and stop and call the degree distribution admissible if the mutual information at the output of the check nodes evolves to 0.99, which corresponds to converging to a bit error probability of around 10^{-5} [4], [28]. We notice that while the experiments with lower thresholds for mutual information may result in divergence, simulations with higher values may extend the runtime unnecessarily. Also if the stability condition is satisfied for a certain degree distribution ensemble, the convergence to zero error probability after decoding to a very small probability of error is verified. We also note that in case the selected degree is not admissible, we choose another degree distribution (satisfying the stability condition) until we obtain an admissible initial degree.

We employ a specific implementation of differential evolution [24] for designing the outer LDPC code. Having obtained the admissible initial degree distributions, we use perturbing vectors to generate a new instance with the goal of maximizing the rate of the code. Both variable node and check node degree distributions are perturbed as $\hat{\lambda}_i = \lambda_i + e_{1i}$, $\hat{\rho}_j = \rho_j + e_{2j}$ where e_{1i} and e_{2j} denote the i th and the j th elements of the perturbing vectors. For the degree distribution to be valid the following equations should be satisfied

$$\sum_{i=2}^{d_v} \lambda_i + e_{1i} = 1, \quad 0 \leq \lambda_i + e_{1i} \leq 1, \quad 2 \leq i \leq d_v, \quad (5)$$

$$\sum_{j=2}^{d_c} \rho_j + e_{2j} = 1, \quad 0 \leq \rho_j + e_{2j} \leq 1, \quad 2 \leq j \leq d_c. \quad (6)$$

At each iteration of the perturbation, we increase the current rate (r) by ΔR , which enforces

$$1 - \frac{\sum_{j=2}^{d_c} \frac{\rho_j + e_{2j}}{j}}{\sum_{i=2}^{d_v} \frac{\lambda_i + e_{1i}}{i}} = r + \Delta R. \quad (7)$$

We draw all the elements of the perturbing vectors except three from a normal distribution $\mathcal{N}(0, \sigma^2)$ where σ is a design parameter [4]. The remaining three elements are obtained via (5)-(7). The perturbed degree distribution replaces the current one if it is admissible, otherwise it is dismissed and a new perturbation is performed. The procedure is terminated if no rate improvement is obtained after a certain number of iterations.

IV. ASYMPTOTIC ANALYSIS OF THE ITERATIVE DECODER

In this section, we derive a stability condition for the iterative decoder, which specifies its convergence behavior when the probability of the decoding error is very small, namely, it shows whether the probability of error will converge to zero or not. Another important consequence of the stability condition is that the implied upper bound on the threshold, in some cases, is tight. Stability condition has been derived for different cases previously, e.g., LDPC codes in P2P scenarios, Gaussian broadcast channels, GICs as well as parallel and serially concatenated turbo codes in [4], [27], [32], and [33], respectively. On the other hand, it is not available for concatenation of LDPC codes with inner trellis-based codes (even in the single user case), which motivates us to derive it for the concatenated coding scheme in a general form, and utilize it in the design of the outer LDPC codes for the specific scenario.

We first go over some definitions and state several propositions that will help in our presentation later in this section. In the following definitions, the term ‘‘mapper’’ refers to a memoryless one-to-one mapper.

Definition 1: The distance spectrum of a codeword is the set of all Hamming distances from that specific codeword to all the other codewords.

Definition 2: A code is called symmetric if the distance spectrum of all of its codewords are the same.

All binary linear codes, specifically, convolutional codes are instances of such symmetric codes.

Definition 3: A one-to-one mapper for which the input labels are the set of all binary sequences of length m_i and the Hamming distance between each pair of the output labels are the same is called *pairwise symmetric*.

An example of a pairwise symmetric mapper is $\{00, 11, 01, 10\} \rightarrow \{100, 010, 001, 111\}$.

Proposition 1: Combination of a convolutional code with a pairwise symmetric mapper is a symmetric code.

The proof is straightforward and follows from the Definitions 2 and 3.

Definition 4: Directional Hamming distance $d_D(\mathbf{c}_1, \mathbf{c}_2) = (d_{01}, d_{10})$ is a pair of distance values for which d_{01} (d_{10}) is the number of positions at which \mathbf{c}_1 has a 0 (or 1) and \mathbf{c}_2 has a 1 (or 0), respectively.

Note that $d_D(\mathbf{c}_1, \mathbf{c}_2)$ is not necessarily equal to $d_D(\mathbf{c}_2, \mathbf{c}_1)$.

Definition 5: A one-to-one mapper for which the input labels are the set of all binary sequences of length m_i and the directional Hamming distance between each pair of the output labels are the same is called *pairwise directional symmetric*.

An example of a pairwise directionally symmetric mapper is $\{00, 11, 01, 10\} \rightarrow \{1000, 0100, 0010, 0001\}$.

Definition 6: A code for which the directional distance spectra of all of the codewords are the same is called *directionally symmetric*.

One may note that the directional symmetry of a code is a stronger property than symmetry.

Proposition 2: Combination of a convolutional code with a pairwise directionally symmetric mapper is a directionally symmetric code.

The proof is straightforward and follows from the Definitions 4, 5 and 6.

A. LLR Symmetry Property

It is shown in [27] that for an output-symmetric channel,¹ the PDFs of the LLRs passed between variable and check node decoders of an LDPC code are symmetric, which simplifies the analysis. On the other hand, an exact analytical investigation of the BCJR decoder regarding the densities of the extrinsic LLRs seems infeasible. For the case of parallel concatenated convolutional codes, the symmetry property for the exchanged extrinsic LLRs between the component decoders is stated as an observation in [28]. Similarly, our extensive large block length simulations show that the symmetry property holds for the proposed concatenated scheme as well (at least approximately), i.e.,

$$\langle f_e(m) \rangle = \frac{f_{e,0}(m) + f_{e,1}(-m)}{2} \quad (8)$$

is symmetric, where $f_{e,0}$ and $f_{e,1}$ denote the codeword averaged LLR densities corresponding to transmitting input bit 0 and 1, respectively.

For the cases of symmetric trellis codes over a symmetric channel or directionally symmetric codes over an asymmetric channel, it is sufficient to use the codeword corresponding to the all-zero message to obtain the average LLR density $\langle f_e(m) \rangle$, which is equal to $f_{e,0}$. For all other cases, one can take an average over a large block length typical codeword with a uniform 0 and 1 distribution to estimate $\langle f_e(m) \rangle$.

Considering that the density evolution equations at the variable and check nodes of the LDPC code preserve the symmetry property [27], the LLR densities at the output of each component decoder will be symmetric as well.

B. Asymptotic Density Evolution for Trellis-Based Codes

An approximate asymptotic density evolution analysis for recursive systematic convolutional codes has been performed in [33]. Inspired by this approach, we analyze the asymptotic behavior of the BCJR decoder for other classes of trellis-based codes on a general asymmetric channel. We consider the case of a non-recursive non-systematic convolutional code plus a

¹By an output symmetric channel we mean that $p(y|x=1) = p(-y|x=-1)$ where $p(y|x=i)$ is the conditional probability of the channel output y given that channel input $x = i$, $i \in \{0, 1\}$.

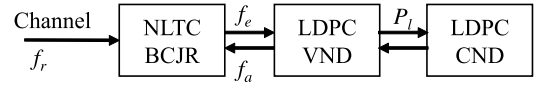


Fig. 3. Iterative decoder for concatenated code.

one-to-one memoryless mapper as the trellis-based code in this analysis. We focus on the case of an asymmetric channel since such channels are observed in multi-user communications, specifically for ICs. We will specialize this analysis to the case of a symmetric channel later in the section.

We consider the general case where each user transmits two messages, one public and one private (\mathbf{x} and \mathbf{u} are the first user's, and \mathbf{v} and \mathbf{w} are the second user's public and private codewords, respectively), and at the receiver side each user decodes three messages. We assume transmission of the randomly selected codewords \mathbf{x}^* , \mathbf{u}^* , \mathbf{v}^* and \mathbf{w}^* (with uniform distribution over their codebooks) and without loss of generality, we study the iterative decoding process for the message $\mathbf{c}(\mathbf{x}^*)$. A BCJR decoder performs decoding over the product trellis of three codes and exchanges soft information with their respective LDPC decoders in an iterative manner. The output of the product trellis \mathbf{q} is a function of the three corresponding codes, i.e., $q_i = f_1(x_i, u_i, v_i)$ and the received channel output is $y_i = f_2(q_i, w_i, z_i)$ where z_i is the realization of the noise random variable at time instant i .

We denote the PDF of the channel LLRs, a priori LLRs from the VND to the BCJR decoder, extrinsic LLRs at the output of the BCJR decoder and the LLRs from VND to CND (at the l th iteration) as f_r , f_a , f_e and P_l , respectively, in which for the first three, the subscript l is dropped, as shown in Fig. 3. We consider the regime where the bit error probability $\mathcal{P}(f_a) \rightarrow 0$. Assuming that the all zero sequence is transmitted,² and 0 bit is mapped to $+1$ and 1 bit is mapped to -1 , we have

$$\mathcal{P}(f) = \int_{-\infty}^0 f(x) dx. \quad (9)$$

The modified LLR at the output of the BCJR decoder corresponding to the k th message bit $c_k(\mathbf{x}^*)$ is defined as $L_k^* = (-1)^{c_k(\mathbf{x}^*)} L_k$, which is given by

$$\begin{aligned} L_k^* &= \log \frac{P(c_k(\mathbf{x}) = c_k(\mathbf{x}^*)|\mathbf{y})}{P(c_k(\mathbf{x}) = 1 - c_k(\mathbf{x}^*)|\mathbf{y})} \\ &= \log \frac{\sum_{\mathbf{x}, c_k(\mathbf{x})=c_k(\mathbf{x}^*)} P(\mathbf{x}|\mathbf{y})}{\sum_{\mathbf{x}, c_k(\mathbf{x})=1-c_k(\mathbf{x}^*)} P(\mathbf{x}|\mathbf{y})}. \end{aligned} \quad (10)$$

Note that L_k^* is the LLR value if the corresponding bit is 0, and it is the negative of the LLR value if the corresponding bit is 1. With the assumption that $\mathcal{P}(f_a) \rightarrow 0$, i.e., high quality a priori information, the summations can be approximated by

²This assumption is valid for the LDPC code by utilizing an i.i.d. random channel adaptor between the outer and the inner code.

maximum operations, namely,

$$L_k^* \simeq \max_{\mathbf{x}, c_k(\mathbf{x})=c_k(\mathbf{x}^*)} \log P(\mathbf{x}|\mathbf{y}) - \max_{\mathbf{x}, c_k(\mathbf{x})=1-c_k(\mathbf{x}^*)} \log P(\mathbf{x}|\mathbf{y}). \quad (11)$$

The first term in this expression (asymptotically) delivers the correct codeword \mathbf{x}^* as $\mathcal{P}(f_a) \rightarrow 0$, hence we can write

$$\begin{aligned} L_k^* &\simeq \log P(\mathbf{x}^*|\mathbf{y}) - \max_{\mathbf{x}, c_k(\mathbf{x})=1-c_k(\mathbf{x}^*)} \log P(\mathbf{x}|\mathbf{y}) \\ &= \min_{\mathbf{x}, c_k(\mathbf{x})=1-c_k(\mathbf{x}^*)} \log \frac{P(\mathbf{x}^*|\mathbf{y})}{P(\mathbf{x}|\mathbf{y})}. \end{aligned} \quad (12)$$

The argument of the log function in the last equation can be rewritten as

$$\begin{aligned} \frac{P(\mathbf{x}^*|\mathbf{y})}{P(\mathbf{x}|\mathbf{y})} &= \frac{\sum_{\mathbf{u}, \mathbf{v}} P(\mathbf{y}|\mathbf{x}^*, \mathbf{u}, \mathbf{v}) P(\mathbf{x}^*) P(\mathbf{u}) P(\mathbf{v})}{\sum_{\mathbf{u}, \mathbf{v}} P(\mathbf{y}|\mathbf{x}, \mathbf{u}, \mathbf{v}) P(\mathbf{x}) P(\mathbf{u}) P(\mathbf{v})} \\ &= \frac{P(\mathbf{y}|\mathbf{x}^*, \mathbf{u}^*, \mathbf{v}^*) P(\mathbf{x}^*)}{P(\mathbf{y}|\mathbf{x}, \mathbf{u}^*, \mathbf{v}^*) P(\mathbf{x})}, \end{aligned} \quad (13)$$

where the last equality is obtained by assuming that the other two codewords (\mathbf{u}^* , \mathbf{v}^*) are decoded completely.

Substituting (13) into (12) we obtain

$$L_k^* \simeq \min_{\mathbf{x}, c_k(\mathbf{x})=1-c_k(\mathbf{x}^*)} \left\{ \log \left(\prod_i \frac{P(y_i|x_i^*, u_i^*, v_i^*)}{P(y_i|x_i, u_i^*, v_i^*)} \times \prod_j \frac{P(c_j(\mathbf{x}^*))}{P(c_j(\mathbf{x}))} \right) \right\} \quad (14)$$

where we use the memoryless channel assumption, and also assume that a priori probabilities of the message bits are independent of each other, i.e., $P(\mathbf{x}^*) = \prod_j P(c_j(\mathbf{x}^*))$.

Note that the minimization in the last expression is over all the paths in the product trellis corresponding to the codewords $\mathbf{x}|_{c_k(\mathbf{x})=1-c_k(\mathbf{x}^*)}$, \mathbf{u}^* and \mathbf{v}^* . Let these paths be denoted by $\mathcal{R}^{k, \mathbf{x}^*, \mathbf{u}^*, \mathbf{v}^*}$. Hence, we can rewrite the last equation as

$$\begin{aligned} L_k^*(x) &\simeq \min_{\mathbf{r} \in \mathcal{R}^{k, \mathbf{x}^*, \mathbf{u}^*, \mathbf{v}^*}} \left\{ \sum_{i: q_i \neq q_i^* = 0} L_{c,i}^*(0) + \sum_{i: q_i \neq q_i^* = 1} L_{c,i}^*(1) \right. \\ &\quad + \sum_{j: c_j(\mathbf{x}) \neq c_j(\mathbf{x}^*) = x} L_{a,j}^*(x) \\ &\quad \left. + \sum_{j: c_j(\mathbf{x}) \neq c_j(\mathbf{x}^*) = 1-x} L_{a,j}^*(1-x) \right\} \end{aligned} \quad (15)$$

$\forall x \in \{0, 1\}$ where $L_{c,i}^*$ and $L_{a,j}^*$ denote the modified channel LLRs and a priori LLRs of the message bits, respectively.

The modified extrinsic LLR $L_{e,k}^*$ corresponding to the k^{th} information bit is given by $L_{e,k}^*(x) = L_k^*(x) - L_{a,k}^*(x)$, hence

$$\begin{aligned} L_{e,k}^*(x) &\simeq \min_{\mathbf{r} \in \mathcal{R}^{k, \mathbf{x}^*, \mathbf{u}^*, \mathbf{v}^*}} \left\{ \sum_{i: q_i \neq q_i^* = 0} L_{c,i}^*(0) + \sum_{i: q_i \neq q_i^* = 1} L_{c,i}^*(1) \right. \\ &\quad + \sum_{\substack{j: c_j(\mathbf{x}) \neq c_j(\mathbf{x}^*) = x \\ j \neq k}} L_{a,j}^*(x) \\ &\quad \left. + \sum_{j: c_j(\mathbf{x}) \neq c_j(\mathbf{x}^*) = 1-x} L_{a,j}^*(1-x) \right\}. \end{aligned} \quad (16)$$

For each $\mathbf{r}_n \in \mathcal{R}^{k, \mathbf{x}^*, \mathbf{u}^*, \mathbf{v}^*}$, we have the input directional distance $d_D(\mathbf{c}(\mathbf{x}^*), \mathbf{c}(\mathbf{x})) = (w_0, w_1)_n$ and output directional distance $d_D(\mathbf{q}^*, \mathbf{q}) = (h_0, h_1)_n$. Hence the asymptotic PDF of the $L_{e,k}^*(x)$ can be obtained using the union bound as

$$\begin{aligned} f_{e,x}^* &= \sum_{n, (w_0, w_1, h_0, h_1)_n} D_n f_{r,0}^{*\otimes(h_0)_n} \otimes f_{r,1}^{*\otimes(h_1)_n} \\ &\quad \otimes f_{a,x}^{*\otimes((w_x)_n-1)} \otimes f_{a,1-x}^{*\otimes(w_{1-x})_n} \end{aligned} \quad (17)$$

where D_n is the number of error paths in $\mathcal{R}^{k, \mathbf{x}^*, \mathbf{u}^*, \mathbf{v}^*}$ with input directional distance $(w_0, w_1)_n$ and output directional distance $(h_0, h_1)_n$. The above expression refers to the PDF of $L_{e,k}^*(x)$ corresponding to the bit x for arbitrary but fixed selection of codewords \mathbf{x}^* , \mathbf{u}^* and \mathbf{v}^* .

The set of error paths $\mathcal{R}^{k, \mathbf{x}^*, \mathbf{u}^*, \mathbf{v}^*}$ in (16) may be different for distinct selection of the codewords. Therefore, we may obtain different PDFs, $f_{e,x}^*$, by considering different codewords being transmitted. Here, as an approximation, we note that using a large block length typical codeword (with a uniform distribution of 0's and 1's at the input), the resulting PDF $f_{e,x}^*$ can be treated as the average of the PDFs over all the codewords. Applying this averaging over all possible selections of \mathbf{x} , \mathbf{u} and \mathbf{v} , the updated expression for the PDF of the modified extrinsic LLRs becomes

$$\begin{aligned} f_{e,x}^* &= \sum_{n, (w_0, w_1, h_0, h_1)_n} p_n D_n f_{r,0}^{*\otimes(h_0)_n} \otimes f_{r,1}^{*\otimes(h_1)_n} \\ &\quad \otimes f_{a,x}^{*\otimes((w_x)_n-1)} \otimes f_{a,1-x}^{*\otimes(w_{1-x})_n} \end{aligned} \quad (18)$$

where p_n is the probability of observing an error path with set of distances $(w_0, w_1, h_0, h_1)_n$.

Assuming transmission of the all-zero codeword for the LDPC code and introducing i.i.d. (random) channel adaptors between the LDPC and trellis-based codes (both at the encoder and decoder sides), the PDF of the modified LLRs at the output of the BCJR decoder becomes the average of $f_{e,x}^*$ for $x = 0, 1$, i.e., $\langle f_e \rangle = \frac{f_{e,0}^* + f_{e,1}^*}{2}$. As a result, the LDPC decoder observes symmetric inputs and the extrinsic LLRs from the LDPC decoder to the BCJR decoder will have the same PDF for $x = 0, 1$, i.e., $f_a = f_{a,0}^* = f_{a,1}^*$. Performing extensive numerical simulations, we have observed that if the corresponding convolutional codes of the trellis-based codes are nonsystematic (which is the case in this paper), then the density of $L_{e,k}^*(x)$ (averaged over a large block length typical codeword) is approximately the same for $x = 0$ and $x = 1$, i.e., $\langle f_e \rangle = f_{e,0} = f_{e,1}^* = f_{e,1}^*$, hence, the symmetric channel assumption for the LDPC code is valid in this case even without using channel adaptors.

C. Asymptotic Density Evolution for the Concatenated Coding Scheme

Assuming that the all-zero codeword for the LDPC code is transmitted, we combine the DE expressions for the LDPC code over a symmetric channel [27] with the average asymptotic density of $\langle f_e \rangle$, and obtain the approximate asymptotic

DE expressions for the concatenated code as follows

$$P_l = \langle f_e \rangle \otimes \lambda \left(\Gamma^{-1}(\rho(\Gamma(P_{l-1}))) \right), \quad (19)$$

$$\langle f_e \rangle = \sum_{n, (w_0, w_1, h_0, h_1)_n} p_n D_n f_{r,0}^{*\otimes(h_0)_n} \otimes f_{r,1}^{*\otimes(h_1)_n} \otimes f_a^{\otimes((w_0)_n + (w_1)_n - 1)}, \quad (20)$$

$$f_a = \tilde{\lambda} \left(\Gamma^{-1}(\rho(\Gamma(P_{l-1}))) \right), \quad (21)$$

where $\tilde{\lambda}(x) = \frac{\int_0^x \lambda(z) dz}{\int_0^1 \lambda(z) dz}$ is the variable node degree distribution

from the node perspective. Since the outgoing message from a variable node towards the BCJR decoder is the summation of all the incoming messages from the check nodes to that variable node, and there is one such message for each variable node, these messages are distributed with respect to $\tilde{\lambda}$ instead of λ . Here, we have considered the inherent cycle-free assumption for the LDPC code, which guarantees the independence of the random variables describing the messages exchanged among the variable and check nodes, and enables us to use the Γ and Γ^{-1} operations over the distributions of the aforementioned random variables [27].

D. Derivation of the Stability Condition

As mentioned in Section IV-A, the average densities are symmetric, therefore instead of looking at the probability of error $\mathcal{P}(P_l)$, we can consider the Bhattacharyya constant of the evolved average densities defined as $\mathcal{B}(P_l) = \int_{-\infty}^{\infty} P_l(x) e^{-x/2} dx$ as a measure of success of the iterative decoding process. Using the Bhattacharyya constant and the derivations in [34, p 234], we can transform the approximate asymptotic density evolution equation into a one-dimensional recursion and obtain the recursive update formula for the Bhattacharyya constant at the variable nodes ($z_l = \mathcal{B}(P_l)$) as

$$z_l \leq \mathcal{B}(\langle f_e \rangle) \lambda(1 - \rho(1 - z_{l-1})) = g(z_{l-1}), \quad (22)$$

$$\mathcal{B}(\langle f_e \rangle) \leq \sum_{n, (w_0, w_1, h_0, h_1)_n} p_n D_n \mathcal{B}^{(h_0)_n}(f_{r,0}^*) \mathcal{B}^{(h_1)_n}(f_{r,1}^*) \times \left(\tilde{\lambda}(1 - \rho(1 - z_{l-1})) \right)^{(w_0)_n + (w_1)_n - 1}. \quad (23)$$

The condition for the fixed point $z_l = 0$ to be locally stable is $\lim_{x \rightarrow 0} \frac{\partial g(z)}{\partial z} < 1$. By evaluating the partial derivative of (22), we see that the terms with $(w_0)_n + (w_1)_n > 1$ will be equal to zero when $z \rightarrow 0$, hence the only terms that remain are for $(w_0, w_1)_n \in \{(0, 1), (1, 0)\}$, which correspond to the paths with a single input bit difference. The resulting stability condition is then

$$d(\mathcal{B}(f_{r,0}^*), \mathcal{B}(f_{r,1}^*)) \lambda'(0) \rho'(1) < 1 \quad (24)$$

where

$$\begin{aligned} d(\mathcal{B}(f_{r,0}^*), \mathcal{B}(f_{r,1}^*)) &= \sum_{\substack{n, (w_0, w_1, h_0, h_1)_n, \\ (w_0, w_1)_n \in \{(0, 1), (1, 0)\}}} p_n \mathcal{B}^{(h_0)_n}(f_{r,0}^*) \mathcal{B}^{(h_1)_n}(f_{r,1}^*) \end{aligned}$$

is the average directional distance spectrum of the paths with a single input bit difference (either 0 to 1 or 1 to 0) over the product trellis of corresponding codes.

Special Case (Single User Decoder): Employing only one message for each user and performing single user decoding at the receiver side, the stability condition is obtained using the same expression as in (24) with the only difference that the function $d(\cdot)$ is the average directional distance spectrum over the single code trellis. Furthermore, if we consider a directionally symmetric trellis-based code, since the directional output distances between any pair of correct and erroneous paths with a single input bit difference are the same (h_0, h_1) , we simply have $d(\mathcal{B}(f_{r,0}^*), \mathcal{B}(f_{r,1}^*)) = \mathcal{B}^{h_0}(f_{r,0}^*) \mathcal{B}^{h_1}(f_{r,1}^*)$.

If the observed channel at the receiver is a symmetric one, the derived stability condition becomes even simpler, and it is given by

$$d(\mathcal{B}(f_r)) \lambda'(0) \rho'(1) < 1 \quad (25)$$

where $d(\mathcal{B}(f_r)) = \sum_i p_i \mathcal{B}^{h_i}(f_r)$ is the average distance spectrum of the paths with a single input bit difference. For the further simplified case of the symmetric trellis-based code since the output distance between any pair of correct and erroneous paths with a single input bit difference is the same (i.e., h is the minimum distance of the code), we simply have $d(\mathcal{B}(f_r)) = \mathcal{B}^h(f_r)$.

By examining the derived stability condition expressions, one might notice that for a given degree distribution there is a threshold for h_0 and h_1 values for which the stability condition is satisfied. Hence, it is required to design an NLTC that satisfies these threshold values. From another perspective, one may notice that having larger h_0 and h_1 values, the set of LDPC degree distributions satisfying the stability condition becomes larger, and hence one has more freedom to design the outer LDPC code (which is performed by searching for an admissible degree distribution with the largest rate or the best threshold within this set).

V. CODE DESIGN EXAMPLES

A. Example 1: One-Sided OR Interference

As the first example of a two-user DMIC, we consider a shared optical channel [8] with one-sided interference, which is an instance of binary-input binary-output Z interference channel (ZIC). The input-output relationship for this channel is given by $Y_1 = (X_1 \otimes X_2) \oplus Z_1$, $Y_2 = X_2 \oplus Z_2$ where \oplus and \otimes represent XOR and OR operations, respectively. Z_1 and Z_2 are the noise samples at receiver 1 and 2 drawn from a Bernoulli distribution with parameters $\epsilon_1 = 0.21$ and $\epsilon_2 = 0.25$, respectively. This model does not satisfy the Markov chain condition for weak interference definition $X_2 - (X_1, Y_2) - Y_1$ [17], however, we can simplify the mutual information condition $I(X_2; Y_1 | X_1) \leq I(X_2; Y_2)$ [17] as

$$P(X_1 = 0) \leq \frac{h(\epsilon_2 + q - 2\epsilon_2 q) - h(\epsilon_2)}{h(\epsilon_1 + q - 2\epsilon_1 q) - h(\epsilon_1)} \quad (26)$$

where $q = P(X_2 = 1)$ and $h(\cdot)$ is the binary entropy function, and verify that for $P(X_1 = 0) < 0.71$ the condition in (26) holds, i.e., the example becomes an instance of the

TABLE I
LABEL ASSIGNMENT TO THE BRANCHES OF 16-STATE TRELLIS ($M = 4$) USING THE ALGORITHM IN [23]

State/Input								y_{21}	y_{22}	y_{23}	y_{24}
0000/0	0001/1	0100/1	0101/0	1010/0	1011/1	1110/1	1111/0	1000	1000	0111	0111
0000/1	0001/0	0100/0	0101/1	1010/1	1011/0	1110/0	1111/1	0100	0100	1011	1011
0010/0	0011/1	0110/1	0111/0	1000/0	1001/1	1100/1	1101/0	0010	0010	1101	1101
0010/1	0011/0	0110/0	0111/1	1000/1	1001/0	1100/0	1101/1	0001	0000	1110	1111

TABLE II
VARIABLE NODE DEGREE DISTRIBUTION OF THE OPTIMIZED CODES FOR EXAMPLE 1 WITH $\epsilon_1 = 0.21$

p_1, p_2	Msg	Rate	λ_2	λ_3	λ_4	λ_9	λ_{10}	λ_{19}	λ_{20}	λ_{49}	λ_{50}
0.5,0.5	X_1	0.0606	0.5149	0.1849	0.0810	0.0336	0.0946	0.0558	0.0312	0.0037	0.0003
	X_2	0.1721	0.3531	0.2408	0.0673	0.0664	0.1503	0.0300	0.0581	0.0093	0.0247
0.5,0.25	X_1	0.1293	0.3523	0.1713	0.1332	0.1198	0.0294	0.0767	0.0237	0.0612	0.0324
	X_2	0.5170	0.4853	0.1141	0.4006						
0.5,0.1875	X_1	0.1523	0.3662	0.1690	0.1411	0.1092	0.0635	0.0585	0.0281	0.0476	0.0168
	X_2	0.3970	0.3737	0.1608	0.4655						
0.5,0	X_1	0.2374	0.3941	0.2023	0.1478	0.1578	0.0590	0.0206	0.0015	0.0037	0.0132

TABLE III
CHECK NODE DEGREE DISTRIBUTION OF THE OPTIMIZED CODES FOR EXAMPLE 1 WITH $\epsilon_1 = 0.21$

p_1, p_2	Msg	Rate	ρ_2	ρ_3	ρ_4	ρ_5	ρ_8	ρ_{14}	ρ_{15}
0.5,0.5	X_1	0.0606	0.0125	0.9875					
	X_2	0.1721		0.0063	0.9710				
0.5,0.25	X_1	0.1293		0.0373	0.9488	0.0139			
	X_2	0.5170	0.0001	0.4016	0.0448		0.0299	0.0348	0.4888
0.5,0.1875	X_1	0.1523		0.0581	0.9135	0.0284			
	X_2	0.3970	0.1020	0.3540	0.0401		0.0426	0.0088	0.4525
0.5,0	X_1	0.2374		0.012809	0.944015	0.043176			

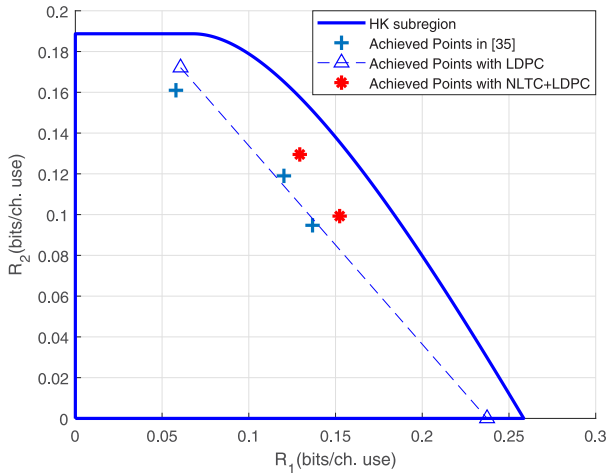


Fig. 4. Rate region and achieved rate pairs for Example 1.

weak interference channel by the definition in [17, Eq. (23)]. Therefore, motivated by the results of [17], we utilize the simple coding scheme of sending the messages of both users as private and compute a subregion of the overall HK ARR.

The achievable HK subregion is plotted for the considered example in Fig. 4. To obtain the largest HK subregion corresponding to each value of $P(X_2) = p_2 \in [0, 1]$ we find the optimal value of $P(X_1) = p_1$ by taking the derivative of mutual information $I(X_1; Y_1)$, and equating it to zero. At the

end, we take the convex hull of all the subregions and obtain the HK subregion corresponding to the use of only private messages.

By calculating the optimal value of p_1 for each $p_2 \in [0, 1]$, we observe that the optimized p_1 is always very close to 0.5, hence we only consider the uniform distribution of zeros and ones for user 1 in this example. To enforce the required non-uniform input distribution for user 2, we design the NLTCs delivering the desired distribution of 0's and 1's. Details of the employed trellis codes are given in Table I with output labels given in columns y_{21} and y_{22} . In each row of the table, the output bits correspond to the input bit u for the current state S . The trellis memory and the number of output bits are both equal to 4, that is, at each section of the trellis, a 1 bit input determines 4-bit outputs. We then optimize the degree distribution of the LDPC codes (with multiple check node and variable node degrees).

The optimized degree distributions are given in Tables II and III. For ones' densities of $p_2 = 0.25$ and 0.1875, the effective rate of the second user's code is the multiplication of the NLTC rate and the LDPC code rate. Fig. 4 shows the optimized rate pairs achieved for different input distributions. As noticed, there is a significant improvement over the results of the previous work in [35]. This improvement is obtained by increasing the memory of the trellis, using multiple check node degrees for LDPC codes, and removing the inner trellis based code for the

TABLE IV
VARIABLE NODE DEGREE DISTRIBUTION OF THE OPTIMIZED CODES FOR EXAMPLE 1 WITH $\epsilon_1 = 0.1$

achieved point	Msg	Rate	λ_2	λ_3	λ_4	λ_5	λ_9	λ_{10}	λ_{19}	λ_{20}	λ_{49}	λ_{50}
*, +	X_1	0.2543	0.4043	0.2482	0.0987		0.1399	0.0363	0.0274	0.0241	0.0079	0.0131
*, Δ	X_2	0.5170	0.4853	0.1141	0.4006							
+, \circ	X_2	0.2422	0.2619	0.4203	0.1729	0.1449						
Δ	X_1	0.3344	0.3478	0.4547	0.0605		0.0567	0.0194	0.0145	0.0034	0.0344	0.0086
\circ	X_1	0.3343	0.3043	0.4528	0.0374		0.0771	0.0472	0.0181	0.0149	0.0162	0.0320

TABLE V
CHECK NODE DEGREE DISTRIBUTION OF THE OPTIMIZED CODES FOR EXAMPLE 1 WITH $\epsilon_1 = 0.1$

achieved point	Msg	Rate	ρ_2	ρ_3	ρ_4	ρ_5	ρ_6	ρ_8	ρ_{14}	ρ_{15}
*, +	X_1	0.2543	0.0217	0.8907	0.0876					
*, Δ	X_2	0.5170	0.0001	0.4016	0.0448			0.0299	0.0348	0.4888
+, \circ	X_2	0.2422	0.0158	0.4996	0.2774			0.0377	0.0615	0.1080
Δ	X_1	0.3344		0.0225	0.6071	0.3704				
\circ	X_1	0.3343		0.0189	0.4980	0.2190	0.2641			

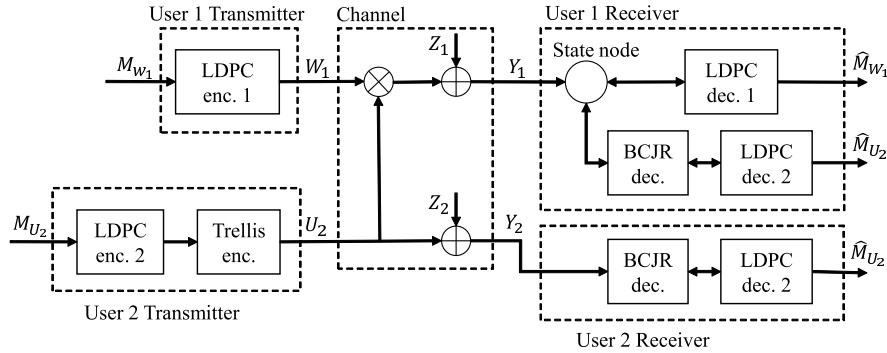


Fig. 5. Block diagram of the proposed coding scheme for Example 1 with $\epsilon_1 = 0.1$ and $\epsilon_2 = 0.25$.

cases of uniform input distribution. According to Fig. 4, the optimized codes offer better performance than single user codes used with time sharing for which the boundary can be obtained by connecting two corner points. It is also worthwhile to mention that, the rate pairs $(0.1293, 0.1295)$, $(0.1523, 0.0993)$, which are obtained with a non-uniform distribution cannot be attained with the joint use of linear coding and time sharing, hence there is a definite need for the use of nonlinear codes.

We next consider the same example with another set of channel parameters, $\epsilon_1 = 0.1$ and $\epsilon_2 = 0.25$. The corresponding HK achievable rate subregions for 1) using only private messages, 2) using private message for the first user and public message for the second one are given in Fig. 6. It can be seen that for this setup, the HK rate subregion can be enlarged by utilizing a public message for the second user. For a specific distribution of the users' messages, namely, $p_1 = 0.5$ and $p_2 = 0.25$, the achievable subregion along with the optimized rate pairs are shown in Fig 6, which illustrates that by utilizing a more sophisticated version of the HK type encoding, namely, private message for one user and public message for the other, we can achieve higher rates compared to the case of using only private messages. Based on this observation, we utilize a simplified version of the proposed general coding scheme where the interfering user's message

TABLE VI
NONLINEAR MEMORYLESS MAPPER WITH RATE $R = 0.5$
AND ONES' DENSITY $p = 0.25$

Input	00	01	10	11
Output	1000	0100	0010	0001

is transmitted as public message and the other user transmits only private message which is illustrated in Fig. 5. As shown in this block diagram, both public message of the second user and private message of the first user are decoded in the first user's receiver. A state node decoder iteratively exchanges messages with the LDPC decoder of user 1 and the BCJR decoder of user 2. We also consider the reference scheme of using a nonlinear memoryless mapper (NLMM) instead of NLTC and optimize the outer LDPC codes for this case as well. The details of the employed NLMM are given in Table VI. This code has a minimum distance of $h = 2$ while the utilized NLTC has a minimum distance of $h = 10$, which provides an advantage in terms of stability and freedom in the outer LDPC code design. The optimal degree distributions for this example are given in Tables IV and V. The achieved rate pairs are depicted in Fig. 6, which shows that considering the public message for the second user, a higher rate for user 1 can be achieved with both the proposed and reference schemes, and

TABLE VII
VARIABLE NODE DEGREE DISTRIBUTION OF THE OPTIMIZED CODES FOR EXAMPLE 2

p_1, p_2	Msg	Rate	λ_2	λ_3	λ_4	λ_9	λ_{10}	λ_{19}	λ_{20}	λ_{49}	λ_{50}
0.5,0.5	X_1	0.095533	0.523868	0.199662	0.071950	0.076520	0.119350	0.003700	0.000850	0.000910	0.003190
	X_2	0.173089	0.349851	0.250499	0.062660	0.064820	0.145850	0.032120	0.065410	0.002540	0.026250
0.5,0.75	X_1	0.148727	0.362650	0.176620	0.117600	0.139440	0.028560	0.089800	0.007230	0.066030	0.012070
	X_2	0.517044	0.485327	0.114083	0.400590						
0.5,0.8125	X_1	0.161381	0.366155	0.160605	0.133580	0.128990	0.051910	0.043150	0.042440	0.032790	0.040380
	X_2	0.398041	0.355933	0.273207	0.370860						
0.5,1	X_1	0.204304	0.378678	0.190902	0.118990	0.153570	0.048290	0.050350	0.042490	0.000570	0.016160

TABLE VIII
CHECK NODE DEGREE DISTRIBUTION OF THE OPTIMIZED CODES FOR EXAMPLE 2

p_1, p_2	Msg	Rate	ρ_2	ρ_3	ρ_4	ρ_5	ρ_8	ρ_{14}	ρ_{15}
0.5,0.5	X_1	0.095533	0.002565	0.978053	0.019382				
	X_2	0.173089	0.002510	0.978166	0.019324				
0.5,0.75	X_1	0.148727		0.013686	0.979620	0.006694			
	X_2	0.517044	0.000130	0.401572	0.044785		0.029873	0.034848	0.488791
0.5,0.8125	X_1	0.161381		0.010969	0.925347	0.063684			
	X_2	0.398041	0.097192	0.379362	0.041831		0.002037	0.005181	0.474396
0.5,1	X_1	0.204304		0.004311	0.917350	0.078339			

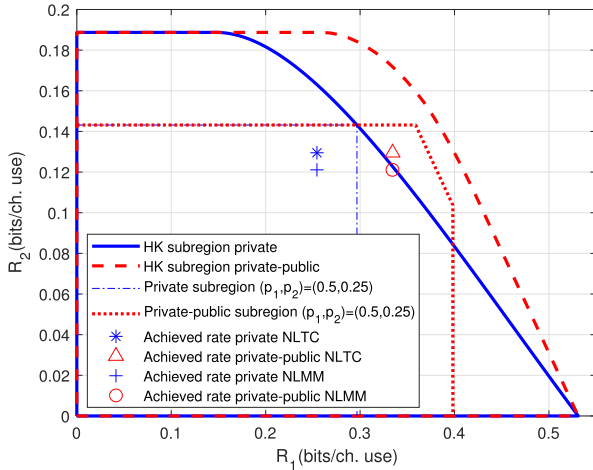


Fig. 6. Rate region and achieved rate pairs for Example 1 with $\epsilon_1 = 0.1$ and $\epsilon_2 = 0.25$.

utilizing the NLTC results in an even more improved rate for the second user.

B. Example 2: One-Sided AND Interference

As a second example, we consider an instance of one-sided weak interference channel given by $Y_1 = (X_1.Y_2) \oplus Z_1$, $Y_2 = X_2 \oplus Z_2$ where “.” is the product operation. Z_1 and Z_2 are independent noise samples at receiver 1 and 2 drawn from a Bernoulli distribution with parameters ϵ_1 and ϵ_2 , respectively. This model satisfies the Markov chain condition for weak interference [17, Definition 2], namely, $X_2 - (X_1, Y_2) - Y_1$, hence the sum rate capacity result [17, Th. 1] holds, and it can be achieved by treating interference as noise and using only private messages. We consider an instance of this model with noise parameters $\epsilon_1 = 0.15$ and $\epsilon_2 = 0.25$, and calculate the HK sub-region by considering only private messages for both users.

TABLE IX
CHANNEL TRANSITION PROBABILITIES FOR EXAMPLE 3

$p(y_1 x_1x_2)$	$y_1 = 0$	$y_1 = 1$	$p(y_2 x_1x_2)$	$y_2 = 0$	$y_2 = 1$
$x_1x_2 = 00$	0.65	0.35	$x_1x_2 = 00$	0.65	0.35
$x_1x_2 = 01$	0.6	0.4	$x_1x_2 = 01$	0.4	0.6
$x_1x_2 = 10$	0.45	0.55	$x_1x_2 = 10$	0.8	0.2
$x_1x_2 = 11$	0.2	0.8	$x_1x_2 = 11$	0.3	0.7

By [17, Th. 1] the sum rate capacity is $C_{sum} = \max_{p(x_1)p(x_2)} \{I(X_1; Y_1) + I(X_2; Y_2)\} \simeq 0.307$. In addition the following simple outer bound from [17],

$$R_1 \leq I(X_1; Y_1|X_2),$$

$$R_2 \leq I(X_2; Y_2),$$

$$R_1 + R_2 \leq I(X_1; Y_1) + I(X_2; Y_2).$$

can be evaluated for this example. Observing that the result of the optimization process for X_1 gives an input distribution very close to uniform, we omit the NLTC for the first user. To enforce the non-uniform distributions needed for the second user, we design the trellis codes given in Table I with output labels y_{23} and y_{24} .

The optimal degree distributions for this example are given in Tables VII and VIII. Fig 7 shows the optimized rate pairs achieved for different degree distributions along with achievable HK subregion and the outer bound (given above). We observe that rate pairs close to the achievable rate subregion boundaries are obtained, which cannot be attained with single user codes or with the use of only LDPC codes with time sharing.

C. Example 3: Two-Sided Interference

The third example that we consider is an instance of a general two-user DMIC with binary inputs and outputs, and

TABLE X
VARIABLE NODE DEGREE DISTRIBUTION OF THE OPTIMIZED CODES FOR EXAMPLE 3

p_1, p_2	Msg	Rate	λ_2	λ_3	λ_4	λ_5	λ_9	λ_{10}	λ_{19}	λ_{20}	λ_{49}	λ_{50}
0.5,1	X_1	0.110559	0.524600	0.219120	0.074740		0.073030	0.102140	0.004670	0.001140	0.000540	0.000020
1,0.5	X_2	0.174376	0.382845	0.159305	0.159760		0.096420	0.076520	0.025900	0.017220	0.075790	0.006240
0.5,0.5	X_1	0.059663	0.493890	0.222140	0.052540		0.061960	0.096370	0.007890	0.034620	0.013480	0.017110
	X_2	0.092509	0.494773	0.262927	0.047850		0.032060	0.119730	0.031560	0.008710	0.000980	0.001410
0.5,0.75	X_1	0.082743	0.496704	0.250046	0.044260		0.009440	0.166620	0.018730	0.004610	0.008260	0.001330
	X_2	0.288224	0.301536	0.203664	0.035540	0.459260						
0.75,0.5	X_1	0.176227	0.226072	0.232578	0.030580	0.510770						
	X_2	0.136389	0.367322	0.138428	0.149760		0.110280	0.032280	0.050580	0.076170	0.053370	0.021810

TABLE XI
CHECK NODE DEGREE DISTRIBUTION OF THE OPTIMIZED CODES FOR EXAMPLE 3

p_1, p_2	Msg	Rate	ρ_2	ρ_3	ρ_4	ρ_5	ρ_8	ρ_{14}	ρ_{15}
0.5,1	X_1	0.110559	0.002061	0.971365	0.026574				
1,0.5	X_2	0.174376		0.057316	0.911938	0.030746			
0.5,0.5	X_1	0.059663	0.014065	0.945768	0.040166				
	X_2	0.092509	0.004952	0.956397	0.038651				
0.5,0.75	X_1	0.082743	0.006185	0.964730	0.029085				
	X_2	0.288224	0.159902	0.282646	0.051625		0.097479	0.179678	0.228669
0.75,0.5	X_1	0.176227	0.219390	0.278422	0.032670		0.078990	0.178584	0.211944
	X_2	0.136389		0.026075	0.951936	0.021989			

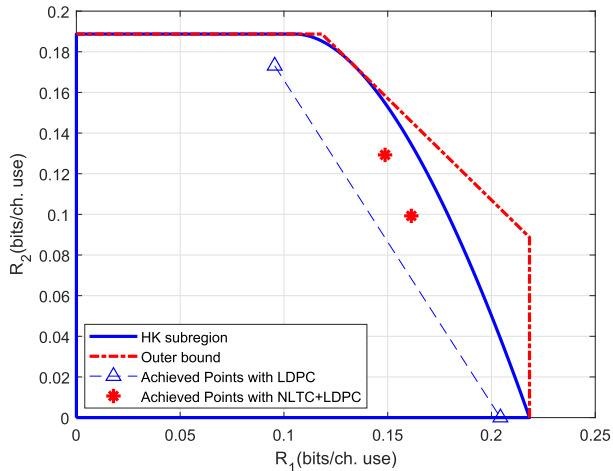


Fig. 7. Rate region and achieved rate pairs for Example 2.

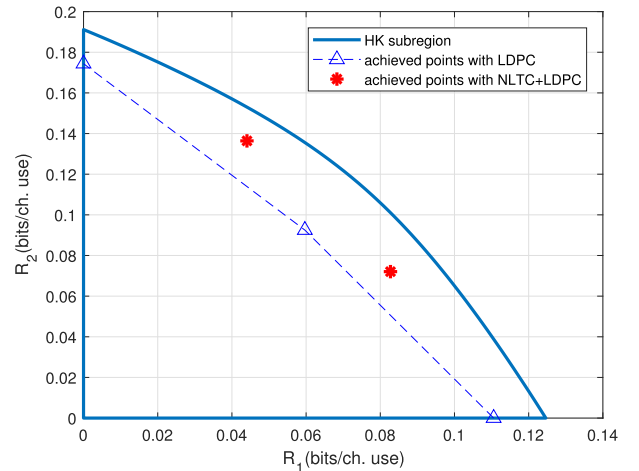


Fig. 8. Rate region and achieved rate pairs for Example 3.

with the channel transition probability given as

$$p(y_1 y_2 | x_1 x_2) = p(y_1 | x_1 x_2) p(y_2 | x_1 x_2), \quad (27)$$

where $p(y_1 | x_1 x_2)$ and $p(y_2 | x_1 x_2)$ are specified in Table IX.

A complete characterization of the HK ARR for this example requires optimization over four random variables with large cardinalities, hence as a simplified version, we consider only private messages and obtain a subregion as illustrated in Fig 8. Note that we employ the NLTC from Example 2 with the ones' density of 0.75 in this example. The degree distributions of the optimized LDPC codes are given in Tables X and XI. The achievable region using only LDPC codes (inducing uniform distribution for both users), and time sharing between them is shown with a dashed line on the same figure. As in the previous examples, it is clear that one can achieve rate pairs that cannot be achieved by linear codes alone.

D. Finite Length Simulation Results

To study the performance of specific codes from the designed ensemble and verify their estimated thresholds, examples of parity check matrices for a block-length of 100k are obtained for the ensembles corresponding to the rate pair (0.1487, 0.1293) with $p_1 = 0.5$ and $p_2 = 0.75$ of Example 2. The parity check matrices are constructed using the tools in [36], which utilize the random construction method. For all cases, 30 decoding iterations are performed. The resulting bit error rates (BERs) are depicted in Fig. 9 showing that the gap between the decoding thresholds and ϵ values for which small error probability is attained is relatively small verifying the accuracy of estimated thresholds. Note that while simulating the user 1's code, the parameter ϵ_2 (which affects the interfering signal) is fixed at the value of 0.25. Furthermore, for user 2, we consider a P2P optimal LDPC

TABLE XII
VARIABLE NODE DEGREE DISTRIBUTION OF THE OPTIMIZED CODES FOR BER SIMULATIONS

	Rate	λ_2	λ_3	λ_4	λ_5	λ_9	λ_{10}	λ_{19}	λ_{20}	λ_{49}	λ_{50}
P2P opt.	0.1293	0.347098	0.194232	0.112600		0.089830	0.073190	0.063250	0.040040	0.060940	0.018820
NLTC opt.	0.4844	0.512632	0.264998	0.072360	0.150010						

TABLE XIII
CHECK NODE DEGREE DISTRIBUTION OF THE OPTIMIZED CODES FOR BER SIMULATIONS

	Rate	ρ_2	ρ_3	ρ_4	ρ_5	ρ_8	ρ_{14}	ρ_{15}
P2P opt.	0.1293		0.043613	0.945854	0.010533			
NLTC opt.	0.4844	0.055807	0.309574	0.120516		0.100152	0.243143	0.170807

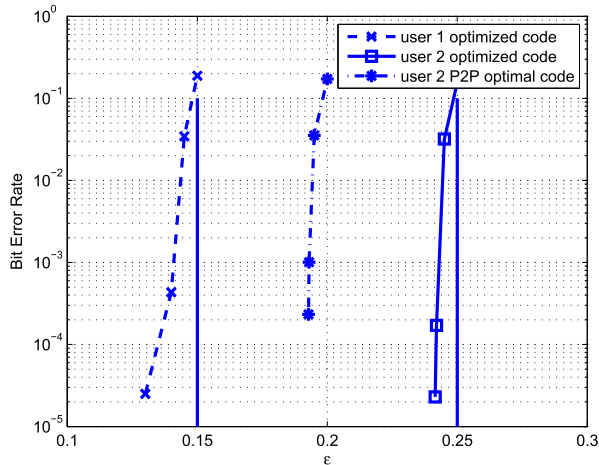


Fig. 9. BER results of Example 2 with $p_1 = 0.5$ and $p_2 = 0.75$.

code instead of the optimized outer LDPC code with the same rate, and obtain the corresponding bit error rates. The degree distributions for the P2P optimal code are given in Tables XII and XIII. We observe that the optimized code for the specific NLTC significantly outperforms the P2P optimal one.

In order to illustrate the advantage of the proposed scheme with respect to the reference of using NLMM in terms of BER, we consider a specific instance (Example 1 with NLMM and NLTC both with ones' density of 0.25). We consider an outer LDPC code optimized for the NLMM with a rate 0.2422, and design another one for the NLTC so that the overall rates for both schemes become identical (i.e., 0.1211). The corresponding degree distributions are given in Tables XII and XIII. We construct parity check matrices with block lengths 10k and 20k for NLTC and NLMM cases, respectively, for fairness (to have the same block length of 40k at the input of the channel). Performing BER simulations at a crossover probability of 0.23 (with 30 decoding iterations), we obtain a bit error rate of 4.6×10^{-6} and 8.9×10^{-4} for the NLTC and NLMM cases, respectively, demonstrating an advantage of more than two orders of magnitude for the scheme with the NLTC. Similar gains are observed for different block lengths as well (not reported here).

VI. CONCLUSIONS

We have considered the Han-Kobayashi coding by using both public and private messages, and have proposed a coding scheme based on a serial concatenation of an NLTC with an outer LDPC code as a solution for transmission over different

classes of DMICs. By approximate analytical derivations, we have investigated the performance of iterative decoding method in the asymptotic region where the probability of decoding error is close to zero, and based on that, we have derived a stability condition for the concatenated coding scheme. Furthermore, we have used an EXIT analysis along with the derived stability condition to design the outer LDPC code.

Our extensive numerical examples demonstrate that the designed codes achieve rate pairs close to the optimal boundary of the HK subregion that cannot be obtained without using nonlinear codes. In addition, the proposed approach for the general instances of DMICs achieves rate pairs that cannot be attained by using linear codes alone with time sharing or the reference scheme of concatenating LDPC codes with nonlinear memoryless mappers. Finite block length simulations verify the accuracy of the estimated thresholds for the designed codes.

REFERENCES

- [1] M. Dabirnia, "Coding schemes for energy harvesting and multi-user communications," Ph.D. dissertation, Dept. Elect. Electron. Eng., Bilkent Univ., Ankara, Turkey, Dec. 2017.
- [2] A. Bennatan, S. Shamai (Shitz), and A. R. Calderbank, "Soft-decoding-based strategies for relay and interference channels: Analysis and achievable rates using LDPC codes," *IEEE Trans. Inf. Theory*, vol. 60, no. 4, pp. 1977–2009, Apr. 2014.
- [3] S. Sharifi, A. K. Tanc, and T. M. Duman, "On LDPC codes for Gaussian interference channels," in *Proc. IEEE Int. Symp. Inf. Theory (ISIT)*, Honolulu, HI, USA, Jun./Jul. 2014, pp. 1992–1996.
- [4] S. Sharifi, A. K. Tanc, and T. M. Duman, "Implementing the Han-Kobayashi scheme using low density parity check codes over Gaussian interference channels," *IEEE Trans. Commun.*, vol. 63, no. 2, pp. 337–350, Feb. 2015.
- [5] A. Vem, Y. C. Huang, K. R. Narayanan, and H. D. Pfister, "Multilevel lattices based on spatially-coupled LDPC codes with applications," in *Proc. IEEE Int. Symp. Inf. Theory*, Honolulu, HI, USA, Jun./Jul. 2014, pp. 2336–2340.
- [6] A. S. S. Cordovil and G. Fraidenraich, "Achieving the sum-rate for symmetric Gaussian interference channels using LDPC codes," in *Proc. 34th Brazilian Telecommun. Signal Process. Symp.*, 2016, pp. 16–20.
- [7] L. Lin, X. Ma, C. Liang, X. Huang, and B. Bai, "An information-spectrum approach to the capacity region of the interference channel," *Entropy*, vol. 19, no. 6, p. 270, 2017.
- [8] M. Griot, A. I. V. Casado, W.-Y. Weng, H. Chan, J. Wang, and R. D. Wesel, "Nonlinear trellis codes for binary-input binary-output multiple-access channels with single-user decoding," *IEEE Trans. Commun.*, vol. 60, no. 2, pp. 364–374, Feb. 2012.
- [9] S.-N. Hong, S. Kim, and N. Lee. (Jun. 2017). "Uplink multiuser massive MIMO systems with low-resolution ADCs: A coding-theoretic approach." [Online]. Available: <https://arxiv.org/abs/1704.03287>
- [10] H. Sato, "On the capacity region of a discrete two-user channel for strong interference (Corresp.)," *IEEE Trans. Inf. Theory*, vol. 24, no. 3, pp. 377–379, May 1978.

- [11] M. Costa and A. El Gamal, "The capacity region of the discrete memoryless interference channel with strong interference (Corresp.)," *IEEE Trans. Inf. Theory*, vol. IT-33, no. 5, pp. 710–711, Sep. 1987.
- [12] R. Benzel, "The capacity region of a class of discrete additive degraded interference channels (Corresp.)," *IEEE Trans. Inf. Theory*, vol. IT-25, no. 2, pp. 228–231, Mar. 1979.
- [13] N. Liu and S. Ulukus, "The capacity region of a class of discrete degraded interference channels," *IEEE Trans. Inf. Theory*, vol. 54, no. 9, pp. 4372–4378, Sep. 2008.
- [14] A. El Gamal and M. Costa, "The capacity region of a class of deterministic interference channels (Corresp.)," *IEEE Trans. Inf. Theory*, vol. IT-28, no. 2, pp. 343–346, Mar. 1982.
- [15] H.-F. Chong and M. Motani, "The capacity region of a class of semi-deterministic interference channels," *IEEE Trans. Inf. Theory*, vol. 55, no. 2, pp. 598–603, Feb. 2009.
- [16] T. Han and K. Kobayashi, "A new achievable rate region for the interference channel," *IEEE Trans. Inf. Theory*, vol. IT-27, no. 1, pp. 49–60, Jan. 1981.
- [17] F. Zhu and B. Chen, "Capacity bounds and sum rate capacities of a class of discrete memoryless interference channels," *IEEE Trans. Inf. Theory*, vol. 60, no. 7, pp. 3763–3772, Jul. 2014.
- [18] B. Xie, M. Griot, A. I. V. Casado, and R. D. Wesel, "Optimal transmission strategy and explicit capacity region for broadcast Z channels," *IEEE Trans. Inf. Theory*, vol. 54, no. 9, pp. 4296–4306, Sep. 2008.
- [19] U. Bhat, D. Fertonani, and T. M. Duman, "New capacity-achieving encoding schemes for degraded binary broadcast channels," in *Proc. IEEE Global Telecommun. Conf. (GLOBECOM)*, Miami, FL, USA, Dec. 2010, pp. 1–5.
- [20] B. Xie, T. A. Courtade, and R. D. Wesel, "Optimal encoding for discrete degraded broadcast channels," *IEEE Trans. Inf. Theory*, vol. 59, no. 3, pp. 1360–1378, Mar. 2013.
- [21] L. Wang and E. Sasoglu, "Polar coding for interference networks," in *Proc. IEEE Int. Symp. Inf. Theory*, Honolulu, HI, USA, Dec. 2014, pp. 1–5.
- [22] M. Zheng, C. Ling, W. Chen, and M. Tao. (May 2017). "A new polar coding scheme for the interference channel." [Online]. Available: <https://arxiv.org/abs/1608.08742>
- [23] M. Dabirnia and T. M. Duman, "On code design for joint energy and information transfer," *IEEE Trans. Commun.*, vol. 64, no. 6, pp. 2677–2688, Jun. 2016.
- [24] R. Storn and K. Price, "Differential evolution—A simple and efficient heuristic for global optimization over continuous spaces," *J. Global Optim.*, vol. 11, no. 4, pp. 341–359, 1997.
- [25] A. El Gamal and Y.-H. Kim, *Network Information Theory*. Cambridge, U.K.: Cambridge Univ. Press, 2011.
- [26] M. Mondelli, S. H. Hassani, and R. Urbanke, "How to achieve the capacity of asymmetric channels," *IEEE Trans. Inf. Theory*, to be published, doi: [10.1109/TIT.2018.2789885](https://doi.org/10.1109/TIT.2018.2789885).
- [27] T. J. Richardson, M. A. Shokrollahi, and R. L. Urbanke, "Design of capacity-approaching irregular low-density parity-check codes," *IEEE Trans. Inf. Theory*, vol. 47, no. 2, pp. 619–637, Feb. 2001.
- [28] S. ten Brink, "Convergence behavior of iteratively decoded parallel concatenated codes," *IEEE Trans. Commun.*, vol. 49, no. 10, pp. 1727–1737, Oct. 2001.
- [29] J. Hou, P. H. Siegel, L. B. Milstein, and H. D. Pfister, "Capacity-approaching bandwidth-efficient coded modulation schemes based on low-density parity-check codes," *IEEE Trans. Inf. Theory*, vol. 49, no. 9, pp. 2141–2155, Sep. 2003.
- [30] J. Hagenauer, "The exit chart—Introduction to extrinsic information transfer in iterative processing," in *Proc. 12th Eur. Signal Process. Conf.*, Vienna, Austria, Sep. 2004, pp. 1541–1548.
- [31] M. Franceschini, G. Ferrari, R. Raheli, and A. Curtoni, "Serial concatenation of LDPC codes and differential modulations," *IEEE J. Sel. Areas Commun.*, vol. 23, no. 9, pp. 1758–1768, Sep. 2005.
- [32] P. Berlin and D. Tuninetti, "LDPC codes for fading Gaussian broadcast channels," *IEEE Trans. Inf. Theory*, vol. 51, no. 6, pp. 2173–2182, Jun. 2005.
- [33] L. Schmitt and H. Meyr, "On the asymptotics of density evolution for iterative (Turbo) decoding," in *Proc. Allerton Conf. Commun., Control, Comput.*, Monticello, IL, USA, 2005, pp. 1–10.
- [34] T. Richardson and R. Urbanke, *Modern Coding Theory*. New York, NY, USA: Cambridge Univ. Press, 2008.

- [35] S. Sharifi, A. K. Tanc, and T. M. Duman, "LDPC code design for binary-input binary-output Z interference channels," in *Proc. IEEE Int. Symp. Inf. Theory (ISIT)*, Hong Kong, Jun. 2015, pp. 1084–1088.
- [36] *IT++ Library*. Accessed: Jul. 22, 2014. [Online]. Available: <http://itpp.sourceforge.net/4.3.1/>



Mehdi Dabirnia (S'15–M'18) received the B.S. and M.S. degrees from University of Tehran, Tehran, Iran, in 2007 and 2010, respectively, and the Ph.D. degree from Bilkent University, Ankara, Turkey, in 2017, all in electrical engineering. He is currently a Post-Doctoral Researcher with the Department of Information and Communication Technologies, Universitat Pompeu Fabra, Barcelona, Spain. His research interests include communication theory, coding theory, and information theory.



A. Korhan Tanc (S'10–M'12) received the Ph.D. degree in electronics and communications engineering from Istanbul Technical University, Istanbul, Turkey, in 2011. From 2012 to 2013, he was a Post-Doctoral Researcher with the School of Electrical, Computer and Energy Engineering, Arizona State University, Tempe, AZ, USA. He is currently an Associate Professor with the Department of Biomedical Engineering, Biruni University, Istanbul, Turkey. His research interests include adaptive signal processing, communication theory, medical imaging, and multichannel processing. He is serving as an Area Editor for *Physical Communication* (Elsevier).



Shahrouz Sharifi received the B.S. degree from the University of Tehran, Tehran, Iran, in 2009, the M.S. degree from the Sharif University of Technology, Tehran in 2011, and the Ph.D. degree from Arizona State University, Tempe, AZ, USA, in 2015, all in electrical engineering. He is currently with Maxlinear, Carlsbad, CA, USA. His research interests include various topics in information theory and wireless communications with a particular focus on coding techniques.



Tolga M. Duman (S'95–M'98–SM'03–F'11) received the B.S. degree from Bilkent University, Ankara, Turkey, in 1993, and the M.S. and Ph.D. degrees from Northeastern University, Boston, MA, USA, in 1995 and 1998, respectively, all in electrical engineering. He was with the School of Electrical, Computer and Energy Engineering (ECEE), Arizona State University, as an Assistant Professor (1998–2004), an Associate Professor (2004–2008) and a Professor (2008–2012). Since 2012, he has been a Professor with the Electrical and Electronics Engineering Department, Bilkent University, and an Adjunct Professor with the School of ECEE, Arizona State University. His current research interests include systems, with particular focus on communication and signal processing, including wireless and mobile communications, coding/modulation, coding for wireless communications, data storage systems, and underwater acoustic communications.

Dr. Duman is a recipient of the National Science Foundation CAREER Award and the IEEE Third Millennium Medal. He served as an Editor of the *IEEE TRANSACTIONS ON WIRELESS COMMUNICATIONS* from 2003 to 2008, the *IEEE COMMUNICATIONS SURVEYS AND TUTORIALS* from 2002 to 2007, the *IEEE TRANSACTIONS ON COMMUNICATIONS* from 2007 to 2012, and *Physical Communication* (Elsevier) from 2010 to 2016. He has been the Coding and Information Theory Area Editor of the *IEEE TRANSACTIONS ON COMMUNICATIONS* since 2011, and an Editor of *IEEE TRANSACTIONS ON WIRELESS COMMUNICATIONS* and the Editor-in-Chief of *Physical Communication* (Elsevier) since 2016.